

RADIO TELEMETRY OF STAGNATION PRESSURE
FROM A WIND TUNNEL MODEL
MAGNETICALLY SUPPORTED IN SUPERSONIC FLOW

By
P. L. Clemens
von Kármán Gas Dynamics Facility
ARO, Inc.
a subsidiary of Sverdrup and Parcel, Inc.

July 1962

FOREWORD

The author wishes to express his appreciation to l'Office National d'Etudes et de Recherches Aeronautiques (ONERA) for permitting use of test facilities and for the co-operation so generously given in assisting with the conduct of the tests described herein. The encouragement of Professor Maurice Roy and the help of Messrs. Delattre, Dubois, and Beaussier of the ONERA are gratefully acknowledged. Thanks are due also to the NATO Advisory Group for Aeronautical Research and Development (AGARD), through whose sponsorship the visits were arranged which made these tests possible.

This report was presented as a paper at the AIEE Summer General Meeting, June 18-22, 1962, Denver, Colorado.

ABSTRACT

During a set of aerodynamic tests in a Mach number 2.4 wind tunnel, it was proven feasible to telemeter stagnation pressure measurements from within a magnetically suspended, ferromagnetic model. State-of-the-art, f-m radio telemetry, developed for hypervelocity range use, was employed. Although data at the outset of each of three trials reflect errors of less than three percent, inordinate frequency vs temperature interactions introduced intolerable shifts in telemeter center frequency as testing progressed. Several methods may be used to reduce these interactions. Magnetogasdynamic effects arising from the use of the magnetic model suspension technique are discussed in an appendix, and are shown to be negligible in most wind tunnel testing.

CONTENTS

	<u>Page</u>
ABSTRACT	iii
SYMBOLS	v
1.0 INTRODUCTION	1
2.0 APPARATUS	
2.1 ONERA Wind Tunnel S. 8	2
2.2 Telemeter.	2
2.3 Receiver and Antenna	3
3.0 CALIBRATION	3
4.0 TESTS AND RESULTS.	5
5.0 DATA ACCURACY.	6
6.0 CONCLUSIONS	7
REFERENCES	9
APPENDIX: A Note on Magnetogasdynamic Effects . . .	11

ILLUSTRATIONS

Figure

1. Pressure Telemeter Circuit	13
2. Variable Capacitance Pressure Transducer	14
3. Pressure Telemeter Disassembled	15
4. Wind Tunnel Model Equipped with Pressure Telemeter.	16
5. Receiver and Antenna Arrangement	17
6. Pressure Telemeter Calibration.	18
7. Pressure Telemeter Temperature Interaction	19
8. Pressure Telemeter Time History	20

SYMBOLS

B	Vector magnetic flux density, gauss (1 gauss = 6.85×10^{-6} lb/amp ft)
f	Frequency, megacycles/sec
j	Vector current density, amperes/ft ²
L	Reference body length, ft
p	Pressure, millimeters of mercury
q	Dynamic pressure, lb/ft ²
s	Magnetic-to-dynamic body force ratio, dimensionless
T	Temperature, degrees Fahrenheit
V	Vector velocity, ft/sec
ρ	Mass density, slugs/ft ³
σ	Electrical conductivity, mho/cm (1 mho/cm = $0.286 \text{ amp}^2\text{sec}/\text{ft}^2\text{lb}$)

1.0 INTRODUCTION

The magnetic support of wind tunnel models is not a new art. A working magnetic model suspension system was first designed and constructed by l'Office National d'Etudes et de Recherches Aeronautiques (ONERA) as early as 1955 (Ref. 1). Subsequent work by the ONERA has improved the dynamic response characteristics of the system (Refs. 2 and 3) and has enabled measurement of aerodynamic forces imposed upon the model (Ref. 4) as they are reflected in the electrical currents necessary to restrain the model.

Magnetic suspension of wind tunnel models is attractive because of the nearness of its approach to the free-flight environment. The flow field surrounding the model is free of the aerodynamic effects induced by the presence of a sting, struts, or other interfering structural supports. Support reactions are absent from the forces imposed upon the model.* If heat transfer studies are to be undertaken, no corrections need be made for heat conducted through support members. If dynamic stability measurements are of interest, magnetic suspension provides elastic restraint in five degrees of freedom. The elasticity of the restraint is adjustable to accommodate the conditions of the test. Either forced oscillation or free oscillation modes of testing may be used.

Although the magnetic support of wind tunnel models may be quite attractive, its value as a test technique can be no greater than will be permitted by the measurements which may be made through its use. As already mentioned, aerodynamic forces experienced by the model have been measured. Accuracies of these measurements have fallen within one-percent limits (Ref. 4). Pressures have been measured by approaching the model with slender probes. Although this method has shown some success in the measurement of model base pressures (Ref. 4), it is always questionable to what degree the probe has distorted the flow field. Also, the fact that the probe must be slender implies poor response to rapidly fluctuating pressures. Of course, this method is useless in the measurement of pressures near the model's stagnation region.

*It might appear that reactions induced by mechanical supports are simply exchanged for magnetogasdynamic force interactions. However, as is shown in the Appendix, magnetogasdynamic force interactions arising out of the use of magnetic model suspension are negligible in ordinary wind tunnel testing.

Manuscript released by author June 1962.

A pressure measuring system contained entirely within the magnetically supported model would overcome these deficiencies of slow response and flow-field interference. Radio-telemetry might then be used to transmit the measurements from within the model to instrumentation equipment located outside the tunnel. A radio-telemetry development project within the von Kármán Gas Dynamics Facility has produced sturdy, miniature, pressure telemeters for use in free-flight models tested in a hypervelocity range (Ref. 5). To examine the feasibility of using these telemeters in magnetically supported, wind tunnel models, a series of tests was conducted in the ONERA supersonic wind tunnel S.8, located at Chalais Meudon, France. To allow an evaluation of the wind tunnel applicability of such telemeters, it was necessary that the model pressure to be telemetered should be one for which theoretical values might accurately be determined. Stagnation pressure satisfied this requirement.

2.0 APPARATUS

2.1 ONERA WIND TUNNEL S.8

The ONERA Wind Tunnel S.8 is a Mach number 2.42 tunnel which operates with atmospheric inlet. The 8-cm by 8-cm test section is of Perspex (Plexiglas) and is outfitted with a five-channel, magnetic model suspension system in the "L" configuration (Ref. 6). Excepting roll, the model is magnetically restrained in all degrees of freedom. During the initiation of flow, the model base is held by a retractable sting. A small cylindrical boss, machined as part of the model's base, is gripped in a sting socket. Once flow has been established the telescoping sting is withdrawn, leaving the model supported magnetically. This procedure is reversed just prior to the cessation of flow. A vacuum system lowers the pressure within the sting socket to reduce the annoying effect of base reaction which occurs when the model is retrieved.

2.2 TELEMETER

The telemeter circuitry and the pressure transducer which were used in the tests were quite similar to those described in Ref. 5. The circuitry appears as Fig. 1. Figure 2 is a drawing of the variable capacitance pressure transducer. This transducer has a quiescent capacitance of some 25 micromicrofarads. A change in applied pressure of 30 psi produces a capacitance excursion of about two micromicrofarads. As shown in Fig. 1, the transducer is made a part of the tank circuit of the radio-frequency oscillator and the pressure which is sensed controls the

frequency at which the circuit oscillates. A capacitor paralleled with the transducer adjusts the transmitter's center frequency. The choice of circuit values shown results in transmission at a center frequency near 86 mc.

Etched, printed circuit boards were used in assembling the circuit components of the telemeter package. The pressure telemeter, removed from a model, appears in Fig. 3. In this figure there can be seen the small tube which led from the pressure transducer to the orifice at the stagnation point on the nose of the model. Potting of the transistor junction in an epoxy resin insured resistance to mechanical shock which might arise should the model be released inadvertently by the magnetic support system. Reference 7 describes the transistor potting technique. The hole and slot arrangement seen in Fig. 3 was provided in order that the coil antenna might radiate from within the ferromagnetic model. When the model was assembled, as in Fig. 4, the axis of the coil antenna was aligned with the axis of the holes.

2.3 RECEIVER AND ANTENNA

The receiver and antenna arrangement which was used in recovering the telemetered stagnation pressure data from the model appears in Fig. 5. A single-turn, loop antenna was placed outside the test section and near the Perspex test section wall. The plane of the antenna was parallel to the direction of airflow. In the early testing, a trimmer capacitor was paralleled with the loop to permit sharp tuning. The low noise level encountered and the high signal strength provided by the telemeter transmitter were found to make this tuning unnecessary. In order to broaden the pass band of the antenna-receiver system, the tuning capacitor was removed. The data presented in this report were collected without the use of the capacitor.

An ONERA, type 1784, frequency modulation receiver was used. Shifts in the frequency of the telemetered signal appeared as changes in the reading of a microammeter at the receiver's discriminator output. Although the bandpass of the receiver was 1.8 megacycles, modulation of the carrier frequency by only some 200 kc was sufficient to drive the microammeter to its full-scale, 50-microampere reading.

3.0 CALIBRATION

During telemeter calibration, pressures ranging from 250 mm of mercury to one atmosphere were applied to the variable capacitance transducer. A regulated vacuum system provided the calibration pressures and a mercurial barometer was used in measuring these pressures.

For each value of applied pressure, the output of the f-m receiver discriminator was read from a microammeter. During a later repetition of calibration, the telemeter frequencies which resulted from application of pressures were also measured, permitting a correlation of oscillator frequency with discriminator output current. In making these frequency measurements, a Gertsch Products, Inc. model FM-1B, direct-reading, VHF frequency meter was used.

The two pressure calibration characteristics appear as Fig. 6. The oscillator frequency vs pressure calibration is quite linear and behaves according to the empirical relationship:

$$f = 85.763 - (2.66 \times 10^{-4})p$$

The slight nonlinearity evident in the current vs pressure plot is attributed to the output characteristic of the receiver. The frequency and current vs pressure characteristics were traversed both in directions of increasing and of decreasing pressure during calibration. Hysteresis was negligible within the limits of precision of the readout apparatus over the range of pressures covered.

Prior hypervelocity range experience with the telemeter circuit had revealed large temperature vs frequency interactions. The telemeter remained at room temperature during the pressure calibrations and these interactions did not appear. Following the wind tunnel testing of the telemeter, a temperature vs frequency calibration was performed in a temperature-regulated test chamber. During this temperature calibration, the transducer pressure remained constant at an atmospheric value which differed from that measured at the time of testing in the wind tunnel. The previously stated expression for frequency as a function of pressure was used in translating the temperature calibration data to accommodate this difference in barometric pressures. The corrected data appear plotted in Fig. 7, and another empirical expression describes the linear dependence of oscillator frequency upon temperature, over the range of interest:

$$f = 86.810 - 0.017T$$

Several of the data points which appear in this temperature vs frequency plot lie rather far from the assumed, straight-line function. This is attributed to insufficient "soaking" time in the test chamber during calibration. That several of the deviant data lie above and several below the characteristic (e. g., points at 50°F and 85°F) is a result of failure to approach each of the calibration points from the same direction (each of the points below room temperature was approached from the low temperature side; those above room temperature were approached from more elevated temperatures).

4.0 TEST AND RESULTS

The telemeter shown in Fig. 3 was installed within the model which appears in Fig. 4 and was arranged so as to transmit stagnation pressure measurements. The model was suspended magnetically in still air within the wind tunnel test section and radio-frequency signals were satisfactorily received from it. The r-f signal strength indicated at the receiver varied widely as the magnetically supported model was rotated slowly in roll. The extremely directional character of radiation from the hole and slot antenna arrangement was responsible for the variations in transmitter-to-receiver coupling which produced these changes in signal amplitude. In spite of wide variations in the strength of the signal, sufficient r-f energy was available to "quiet" the f-m receiver and produce proper discriminator operation, regardless of the angular orientation of the model.

With the model supported by the retractable sting, the magnetic field strength was varied in order to examine any possible influence of the suspension system upon the telemetered measurement. The magnetic field intensity was varied from zero to roughly twice the value required to support the model without airflow. This variation in magnetic field intensity produced no discernible change in r-f signal amplitude at the receiver. Discriminator output current (hence, telemetered pressure) was similarly unaffected.

The design of the model did not suit it well to testing in the ONERA Wind Tunnel S. 8. Model diameter (3.8 cm) was greater than that intended for use in the tunnel S. 8 test section. As a result, tunnel performance was marginal and "choking" occasionally occurred during the tunnel starting process (i. e., supersonic flow was not consistently established). Model length was such that bow wave reflections from the test section walls impinged upon the afterbody, lessening system stability. Although testing was rather precarious as a result of the inappropriate model design, conditions of the test nonetheless were adequate to allow the collection of stagnation pressure data during each of several brief tunnel runs.

Calibration (Fig. 6) had indicated that the output current supplied by the receiver discriminator was to diminish as telemetered pressure was reduced from atmospheric value to the stagnation value anticipated. Therefore, prior to each test, receiver tuning was offset to produce a

discriminator microammeter reading of $43.5\mu\text{a}$. * Immediately upon establishment of supersonic flow through the tunnel test section, discriminator current was read. Additional current readings were taken at five-second intervals.

Telemetered data collected during three trials appear plotted as Fig. 8. During runs numbered one and two, some 8 to 15 seconds were consumed in releasing the model from its sting support and establishing magnetic suspension. During the run numbered three, the model was supported by the sting throughout the thirty-second interval of data recording. Frequency data plotted in Fig. 8 were derived from the calibration characteristics of Fig. 6.

5.0 DATA ACCURACY

Data representing telemeter performance during the three runs (Fig. 8) show agreement among themselves which is reasonable within the limits of precision of the apparatus used. Data representing stagnation pressure are in perfect agreement at the outset of each run. The very severe temperature sensitivity of the telemeter was circumvented at the start of each run by allowing a period of "soaking" at a room temperature equalling that at the time of pressure calibration. As each trial progressed, telemeter frequency was seen to increase. There is no reason to believe that model stagnation pressure might have varied during the course of each run. Assuming stagnation pressure to have remained constant, the calibration curve of Fig. 7 shows that declining telemeter temperature should have produced an increase in telemeter frequency. The decreasing telemeter temperature, which resulted in the progressively increasing frequency, was to have been expected on the basis of aerodynamic considerations.

*This is the value of discriminator current which resulted from application of atmospheric pressure to the telemeter (Fig. 6) with receiver center frequency having been previously adjusted to produce zero discriminator current upon the application of the arbitrary zero reference pressure of 250 mm Hg. As frequency calibration of the telemeter was to show later, the $43.5\mu\text{a}$ value of discriminator current at atmospheric pressure corresponded to a telemeter oscillator frequency of 85.562 mc. This same, later, frequency calibration indicated that offsetting of the receiver tuning to produce the $43.5\mu\text{a}$ value of discriminator current placed receiver center frequency at a value of 85.697 mc, also corresponding to the arbitrary zero reference of 250 mm Hg.

The 11.7- μ a value of discriminator current read at the initiation of flow during each of the three trials (Fig. 8) corresponds to a pressure of 415 mm Hg, as read from the calibration curve of Fig. 6. The theoretical stagnation pressure, computed through the use of Ref. 8, is 404 mm Hg. An error of 2.73 percent is implied.

Several significant sources of error merit consideration. Resolution of the meter used in monitoring discriminator output current did not exceed 0.5 percent of full-scale value, and the total meter excursion, from atmospheric pressure to measured pressure, was scarcely more than 60 percent of full scale. As a result, one might reasonably expect to encounter errors as great as one percent in the reading of the discriminator current meter alone. As has been shown, temperature influence upon readout was severe. The temperature-induced change in oscillator frequency during a typical, 30-second run was some 41 kc. The total frequency excursion from atmospheric pressure to measured stagnation pressure at the commencement of each run was little more than twice that value (92 kc). Stated otherwise a temperature interaction of some 44 percent occurred during each 30-second run. Further, the temperature calibration curve (Fig. 7) shows that a temperature excursion of only 2.4°F would have been sufficient to produce the frequency shift seen during the course of each run. No attempt has been made to compute theoretical values of telemeter temperature as a function of time. Oscillator frequency is known as a function of temperature only for cases wherein the temperature of the entire telemeter was uniform. Unquestionably, temperature gradients were induced within the circuitry during testing in the tunnel. Therefore, were theoretical values of telemeter temperature to be computed, no reasonable correlation with the temperature calibration could be expected.

In view of the sources of error which existed, it is inconceivable that errors as small as three percent might have been expected from the measuring system. It can only be assumed that some fortuitous combination of compensating errors must have been present.

6.0 CONCLUSIONS

Frequency-modulation radio telemetry of pressure measurements is possible from within a magnetically suspended, ferromagnetic, wind tunnel model undergoing supersonic testing. For telemeter circuits of the type described here, and operating in the region of the frequency spectrum near 86 mc, neither the frequency nor the absolute signal level of the f-m transmission is affected by the introduction of a direct magnetic

field of intensity sufficient to support and restrain the model within supersonic flow. Similarly, alterations in intensity of the supporting magnetic field, from zero to twice the value required to restrain the model, have no discernible effect upon either absolute signal level or center frequency position. Within the limits of resolution of the measuring system used here, repeated aerodynamic tests under identical conditions produced identical results.

Although state-of-the-art radio telemeters developed for hypervelocity range use are applicable to measurements of pressures exerted upon magnetically suspended models, inordinate temperature interactions render use of these telemeters inconvenient. Any of several schemes might reduce these temperature effects:

1. The bandpass of the f-m receiver used during these tests was nearly two megacycles. Total frequency excursion produced by the telemeter was less than 0.1 mc. Modulation over a wider frequency range would better exploit the bandpass of the receiver and would render temperature interactions less significant. However, only those temperature interactions not inherent in the transducer itself could be lessened in this manner.
2. Stabilization of oscillator center frequency through the use of a crystal and its associated circuitry, as suggested in Ref. 9, could be expected to reduce temperature influences. Although the crystal itself would introduce temperature effects, these would be significantly less than those experienced with the system used in the testing described here. Again, only temperature interactions originating outside the transducer would be reduced.
3. Thermistor compensation for temperature interactions, as described in Ref. 10, would introduce negligible circuit complication and could be expected to provide correction of temperature effects whether they were of transducer or of circuit origin.

REFERENCES

1. Tournier, M., Dieulesaint, E., and Laurenceau, P. "Etude, Realisation et Mise au Point d'une Suspension de Maquette Aerodynamique par Action Magnetique pour une Petite Soufflerie (Study, Realization, and Adjustment of a Magnetic Suspension System for Aerodynamic Models in a Small Wind Tunnel)." O.N.E.R.A. N.T. 1/1579 AP.
2. Laurenceau, P. "Etude, Realisation et Mise au Point d'une Suspension de Maquette Aerodynamique par Action Magnetique pour une Petite Soufflerie (Study, Realization, and Adjustment of a Magnetic Suspension System for Aerodynamic Models in a Small Wind Tunnel)." O.N.E.R.A. N.T. 2/1579 AP.
3. Tournier, M. and Laurenceau, P. "Perfectionnements a la Suspension Magnetique des Maquettes (Improvement in the Magnetic Suspension of Models)." O.N.E.R.A. N.T. 5/1579 AP, December 1956.
4. Laurenceau, P. and Desmet, E. "Adaptation de la Suspension Magnetique des Maquettes aux Souffleries S. 19 et S. 8 LCh (Adaptation of Magnetic Suspension of Models to Wind Tunnels S. 19 and S. 8)." O.N.E.R.A. N.T. 7/1579 AP, January 1957.
5. Lukasiewicz, J., Stephenson, W. B., Clemens, P. L., and Anderson, D. E. "Development of Hypervelocity Range Techniques at Arnold Engineering Development Center." AEDC-TR-61-9, AD 258782, June 1961.
6. Desmet, E. and Rosset. "Caracteristiques et Notice d'Emploi de la Suspension Magnetique Destinee aux Souffleries S. 19 et S. 8 (Characteristics and Review of the Use of the Magnetic Suspension System Designed for Wind Tunnels S. 19 and S. 8)." O.N.E.R.A. N.T. 9/1579 AP.
7. Kingery, M. K. "Preliminary Development of Telemetry for Aeroballistic Ranges." AEDC-TN-59-7, AD 208692, February 1960.
8. Ames Research Staff. "Equations, Tables, and Charts for Compressible Flow." NACA Report 1135, 1953.
9. Beaussier, J. "Telemesure pour Maquette Suspendue Magnetiquement en Soufflerie (Telemetry for a Magnetically Suspended Model in a Wind Tunnel)." O.N.E.R.A., La Recherche Aeronautique, No. 82, Mai-Juin 1961.

10. Kingery, M. K. and Clemens, P. L. "An Assessment of Readout Errors Encountered in Radio Telemetry from Gun-Launched Hypervelocity Projectiles." AEDC-TN-61-58, AD 256778, May 1961.
11. Resler, E. L., Jr. and Sears, W. R. "The Prospects for Magneto-Aerodynamics." Journal of the Aeronautical Sciences, Vol. 25, No. 4, April 1958, pp. 235-245, 258.
12. Resler, E. L., Jr., and Sears, W. R. "The Prospects for Magneto-Aerodynamics - Correction and Addition." Journal of the Aero Space Sciences, Vol. 26, May 1959, p. 318.
13. Brunner, M. J. "The Effects of Hall and Ion Slip on the Electrical Conductivity of Partially Ionized Gases for Magnetohydrodynamic Re-Entry Vehicle Application." General Electric Co., ASME Paper No. 61-WA-176, November 1961.

APPENDIX

A NOTE ON MAGNETOGASDYNAMIC EFFECTS

It would appear that the intense magnetic fields required to support and restrain a wind tunnel model might introduce intolerable magnetogasdynamic effects. The advantages gained toward free-flight simulation by the elimination of structural supports might well be lost if fields as intense as the required 6000 to 12,000 gauss were to render the testing aerodynamically unrealistic.

Figure A-1, adapted from Refs. 11 and 12, presents magnetogasdynamic force interactions for real flight through a magnetic field of 10,000 gauss. Relatively large values of force interaction seen here would seem to limit the applicability of the technique. However, absolute temperatures and velocities encountered in real flight are substantially higher than those customarily found in wind tunnel testing. (Wind tunnel work ordinarily seeks to duplicate only Mach numbers and unit Reynolds numbers found in real flight.) Since gaseous electrical conductivity increases with temperature, and electric body force increases with both conductivity and velocity, the outlook for wind tunnel applicability of magnetic model suspension is not nearly so dismal as Fig. A-1 might seem to indicate.

Proceeding from work presented in Ref. 11, an approximate ratio of electric body force (e. b. f.) to aerodynamic body force is determinable:

$$S = \frac{\text{e. b. f.}}{\text{dynamic force}} = \frac{jB}{\frac{1}{2}\rho v^2/L}$$

It is reasonable to assume that current density, j , is equal to σVB . The substitution leads to:

$$S = \frac{\text{e. b. f.}}{\text{dynamic force}} = \frac{\sigma VB^2L}{\frac{1}{2}\rho v^2} = \frac{\sigma VB^2L}{q}$$

This relationship has been applied to a typical family of wind tunnels - those of the von Kármán Facility. In computing the magnetogasdynamic force interactions, representative values of electrical conductivity, based upon temperature, were selected from data presented in Refs. 11 and 13. In order that results be kept conservative (i. e., electric force interactions not be under-estimated), conductivity values were selected on the basis of theoretical stagnation temperatures. Also in order to produce conservative rather than optimistic interaction values, a field intensity of 12,000 gauss was assigned and free-stream velocity figures were used throughout.

The calculations just described have shown that in ordinary wind tunnel testing, at flow velocities lower than 7000 ft/sec, magnetogasdynamic force interactions should not be expected to exceed 0.001 per cent. Testing in hypervelocity, low density tunnels at flow velocities as high as 10,000 ft/sec, might be expected to produce interactions of 0.001 to 1.0 percent. Testing in arc-driven, hotshot tunnels, with flow velocities near 10,000 ft/sec, could result in force interactions of one to ten percent. It is unlikely, however, that magnetic model suspension in its present state of development is applicable to use in hotshot tunnels, where rates of load application are several orders of magnitude greater than those found in more conventional test units.

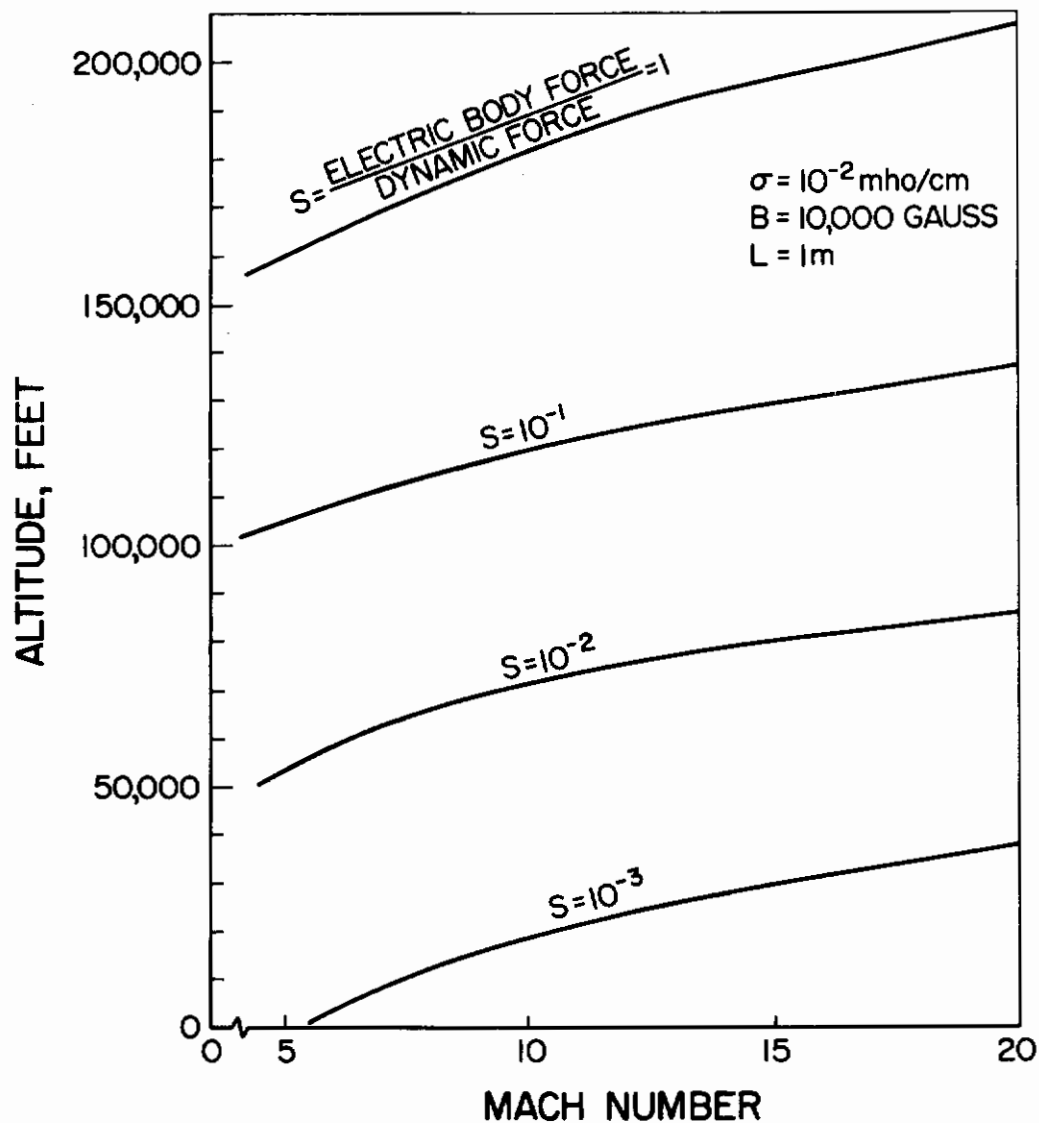


Fig. A-1 Magnetogasdynamic Force Interactions in Real Flight

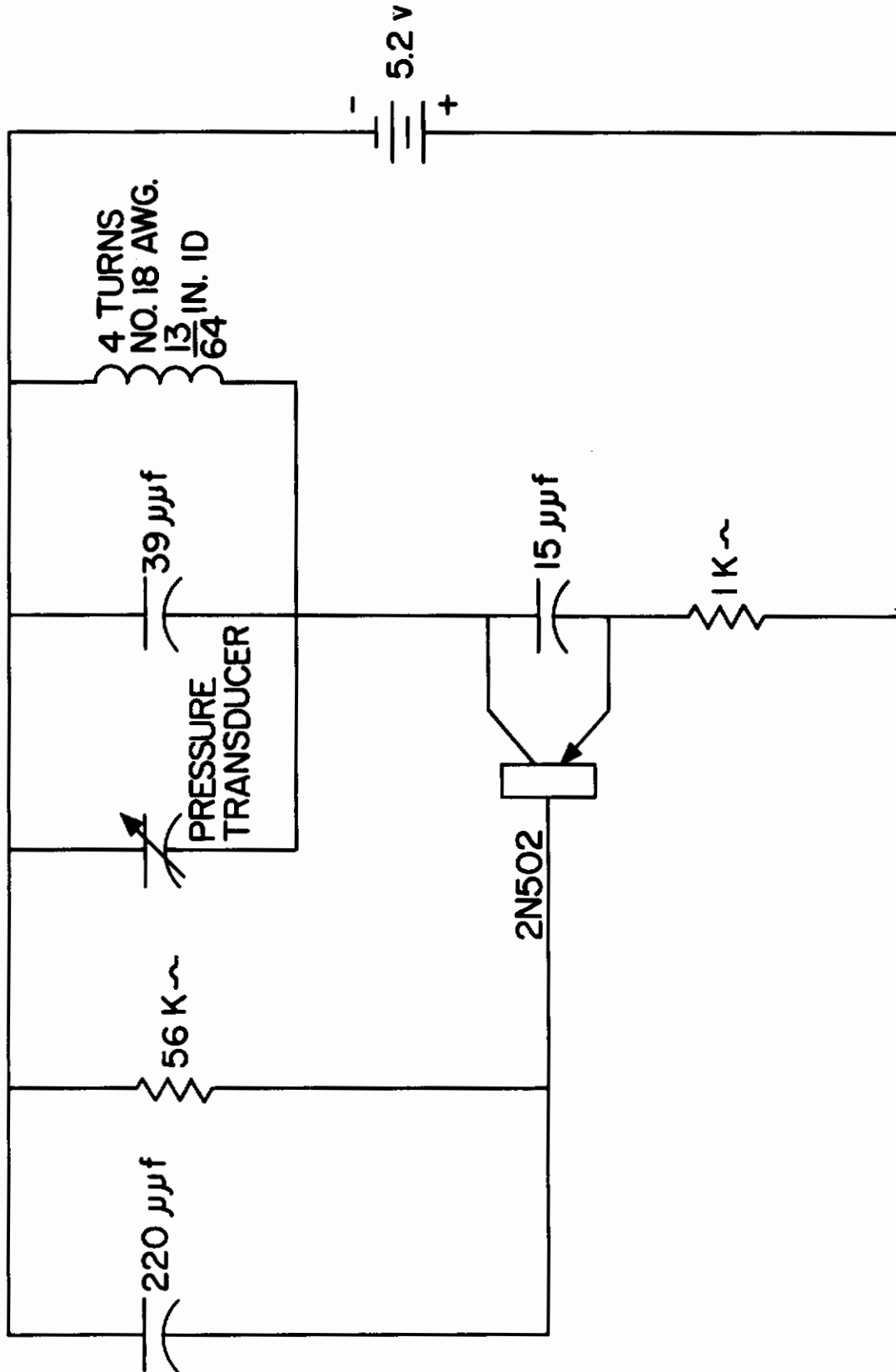


Fig. 1 Pressure Telemeter Circuit

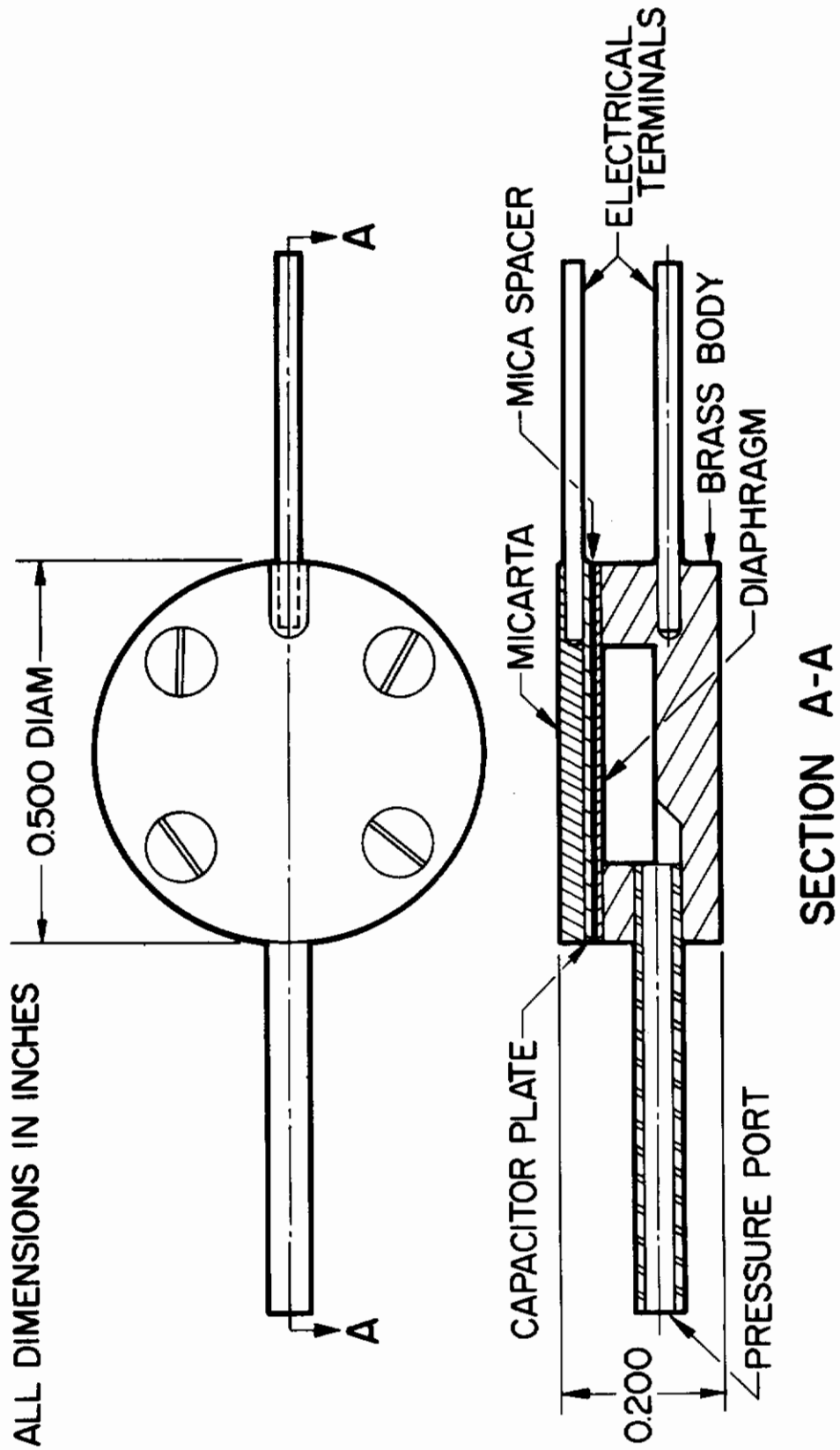


Fig. 2 Variable Capacitance Pressure Transducer

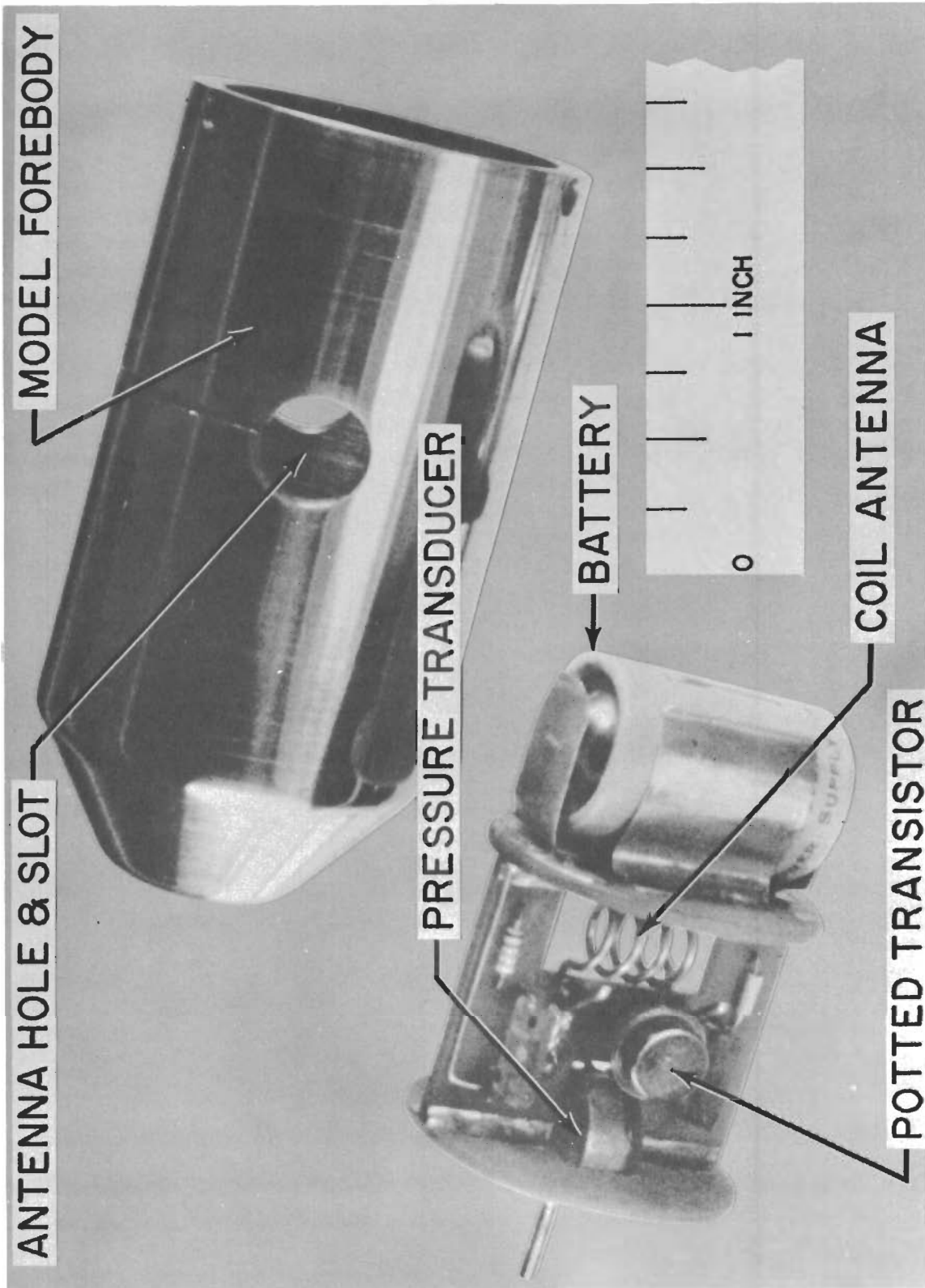


Fig. 3 Pressure Telemeter Disassembled

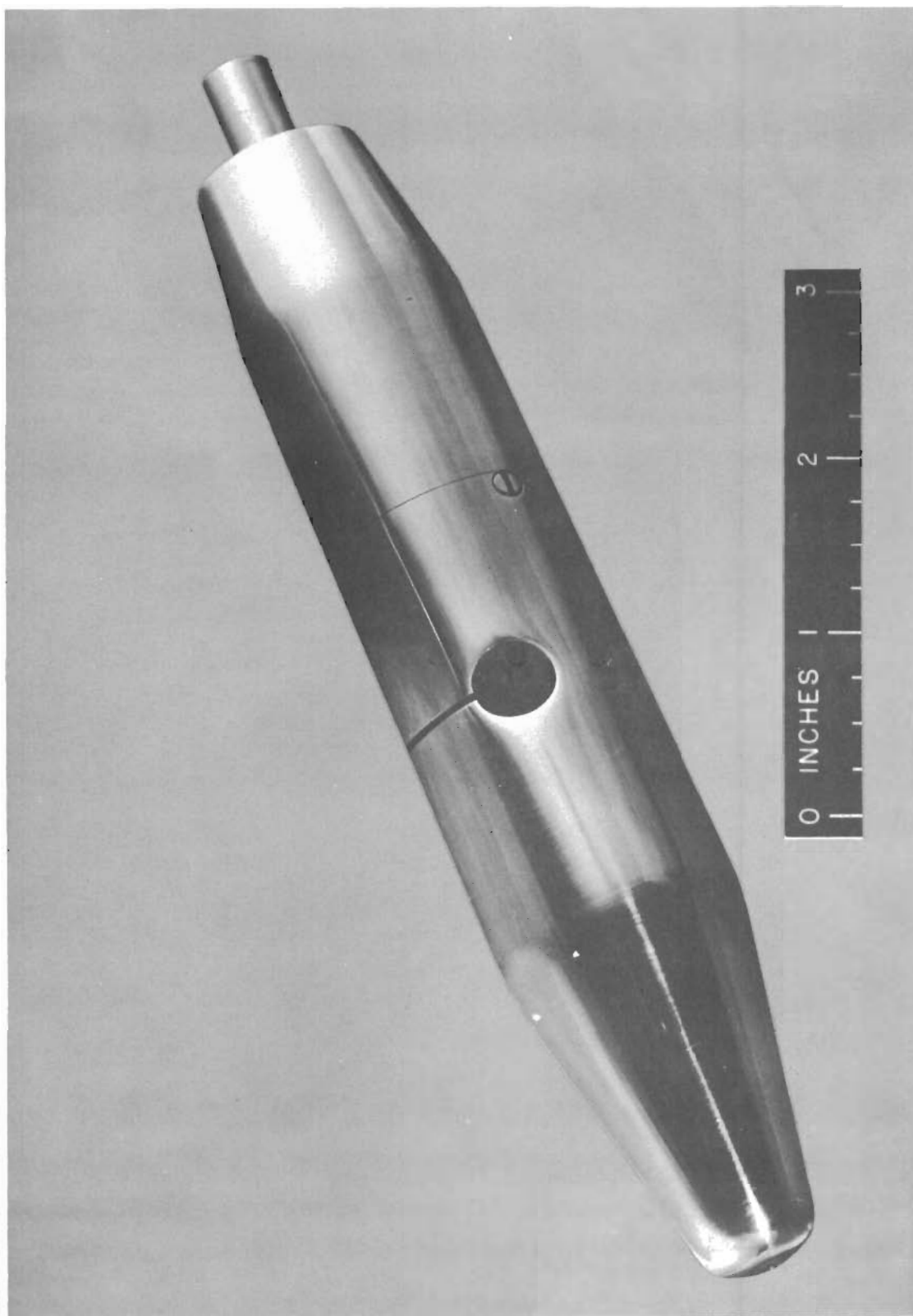


Fig. 4 Wind Tunnel Model Equipped with Pressure Telemeter

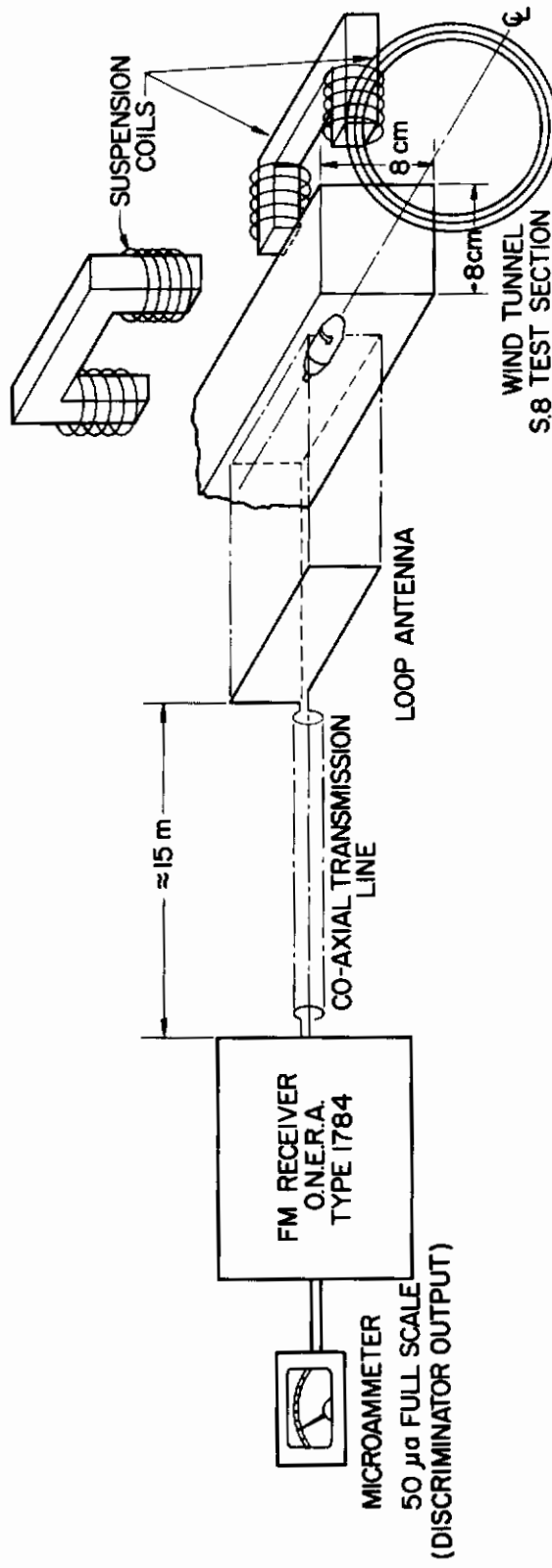


Fig. 5 Receiver and Antenna Arrangement

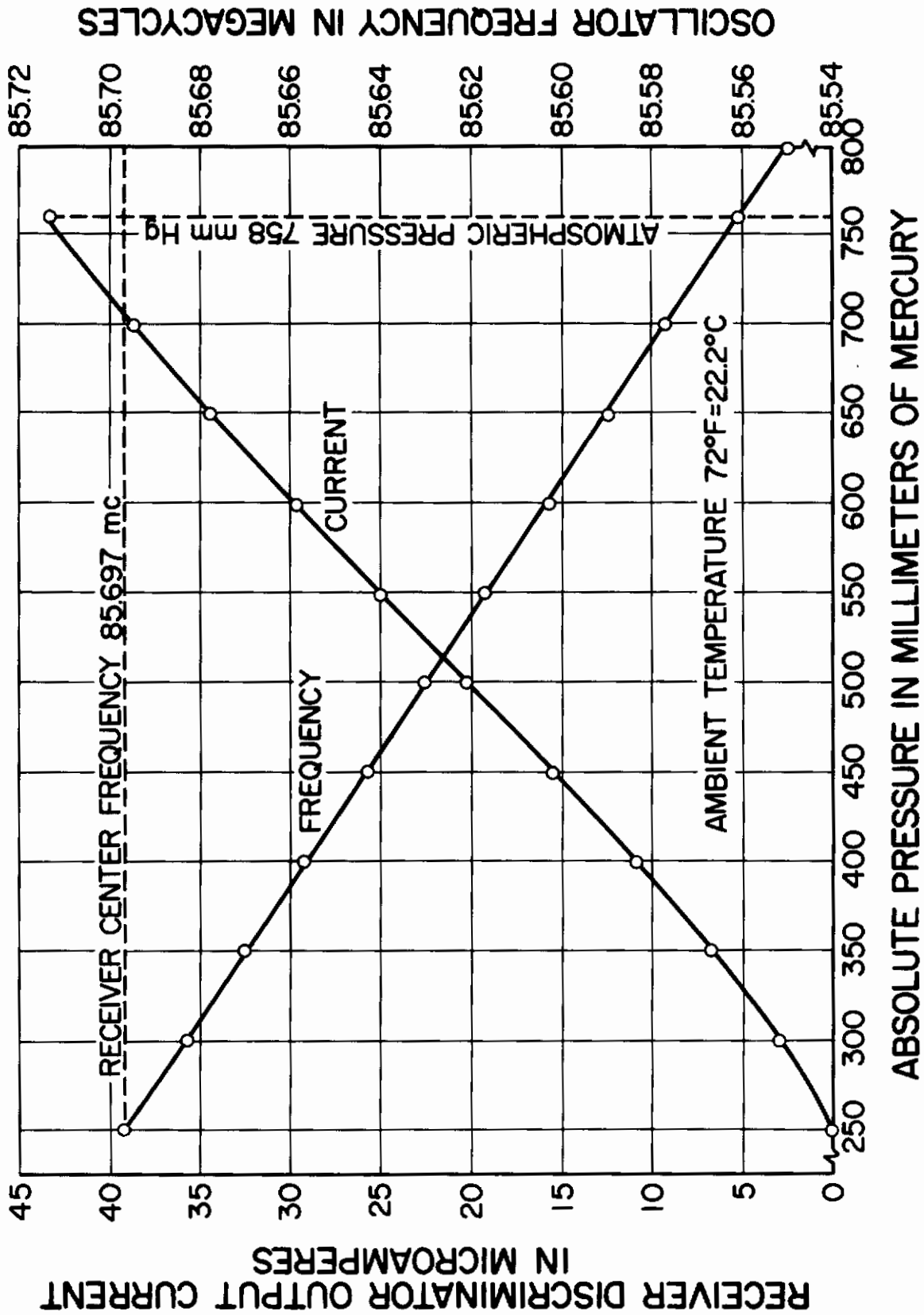


Fig. 6 Pressure Telemeter Calibration

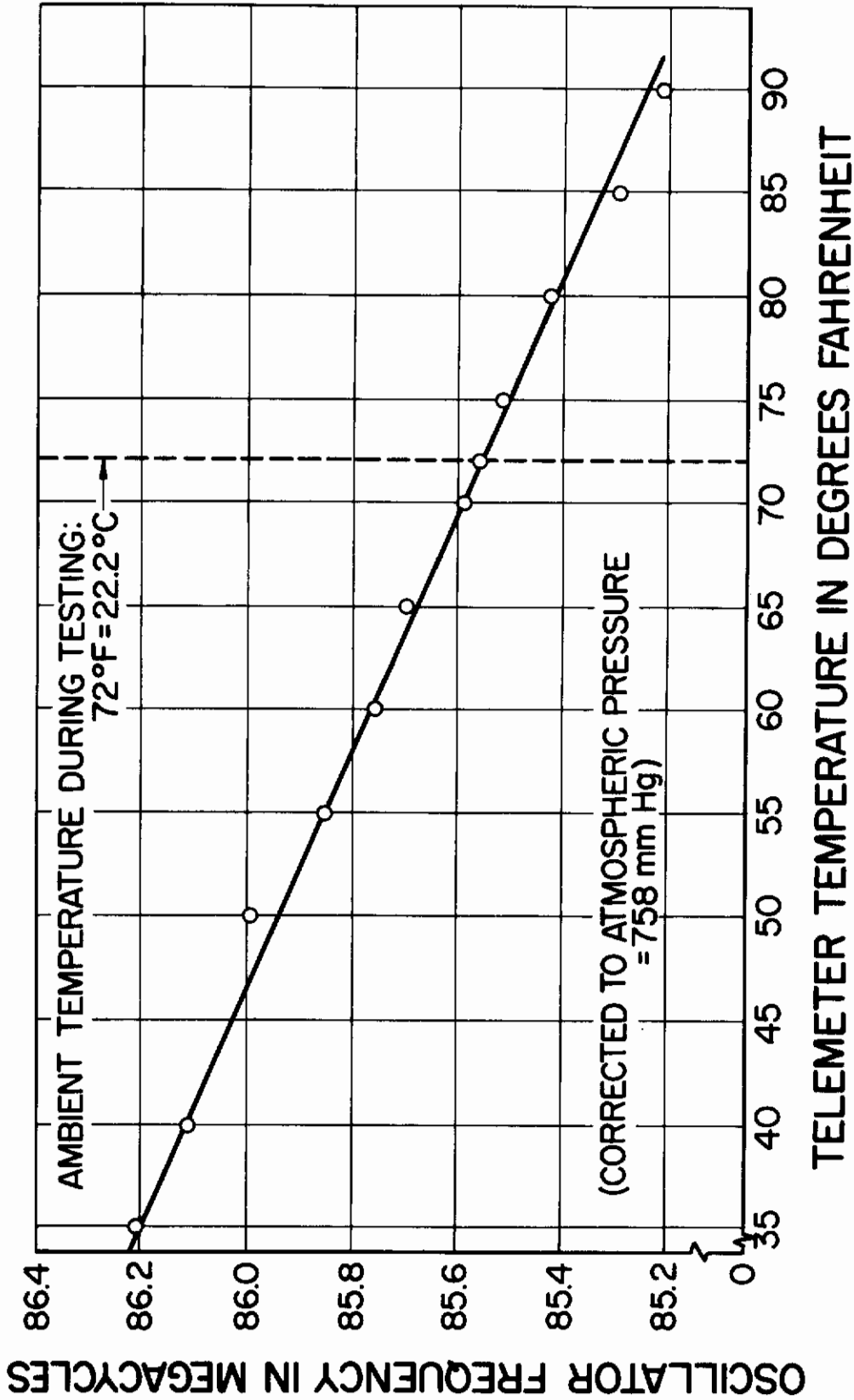


Fig. 7 Pressure Telemeter Temperature Interaction

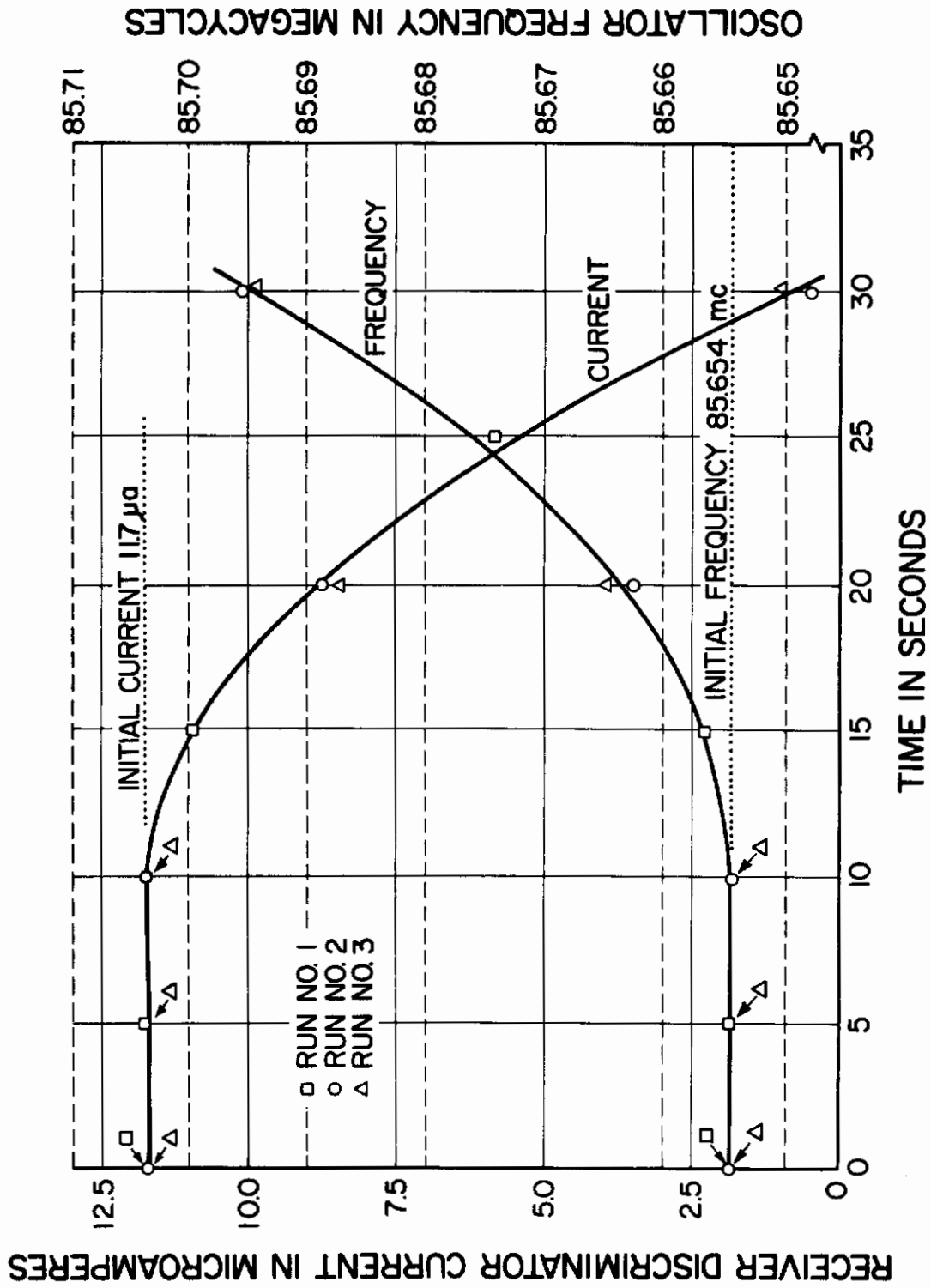


Fig. 8 Pressure Telemeter Time History